Supporting Information

Heterometallic Coordination Polymers Assembled from Trigonal Trinuclear Fe_2Ni-Pivalate Blocks and Polypyridine Spacers: Topological Diversity, Sorption and Catalytic Properties

Svetlana A. Sotnik,[†] Ruslan A. Polunin,[†] Mikhail A. Kiskin,*,[‡] Alexander M. Kirillov,[§] Victoria N. Dorofeeva,[†] Konstantin S. Gavrilenko,[‖],[⊥] Igor L. Eremenko,[‡] Vladimir M. Novotortsev,[‡] and Sergey V. Kolotilov*,[†]

[†] L. V. Pisarzhevskii Institute of Physical Chemistry of the National Academy of Sciences of the Ukraine, Prospekt Nauki 31, Kiev 03028, Ukraine

[‡] N. S. Kurnakov Institute of General and Inorganic Chemistry, Russian Academy of Sciences, Leninsky Prosp. 31, 119991 GSP-1 Moscow, Russian Federation

[§] Centro de Química Estrutural, Complexo I, Instituto Superior Técnico, Universidade de Lisboa, Av. Rovisco Pais, 1049-001 Lisbon, Portugal

[‖] Research-And-Education ChemBioCenter, National Taras Shevchenko University of Kyiv, Chervonotkackaya str., 61, Kiev 03022, Ukraine

[⊥] Enamine Ltd., A. Matrosova str. 23, Kiev 01103, Ukraine

Selected NMR data.

L^3

^{1}H NMR (δ, ppm): 8.38 m (2H, H_5, 3py); 8.70 d (2H, J = 6 Hz, H_3, 4py); 8.74 s (2H, H_3, central py); 9.01 d (2H, J = 6 Hz, H_4, 3py); 9.10 d (2H, J = 6 Hz, H_2, 4py); 9.57 d (2H, J = 8 Hz, H_6, 3py); 9.91 s (2H, H_2, 3py).

L^5

^{1}H NMR (400 MHz, DMSO-d_6): δ_H = 1.17 (t, 6H, J = 7 Hz, $2CH_3$); 3.45 (q, 4H, J = 7 Hz, $2CH_2$); 6.83 (d, 2H, J = 8.6 Hz, Ar); 7.96 (d, 2H, J = 8.6 MHz, Ar); 8.32 (d, 4H, J = 9 Hz, Ar); 8.34 (s, 2H, Ar); (d, 4H, J = 9 Hz, Ar).

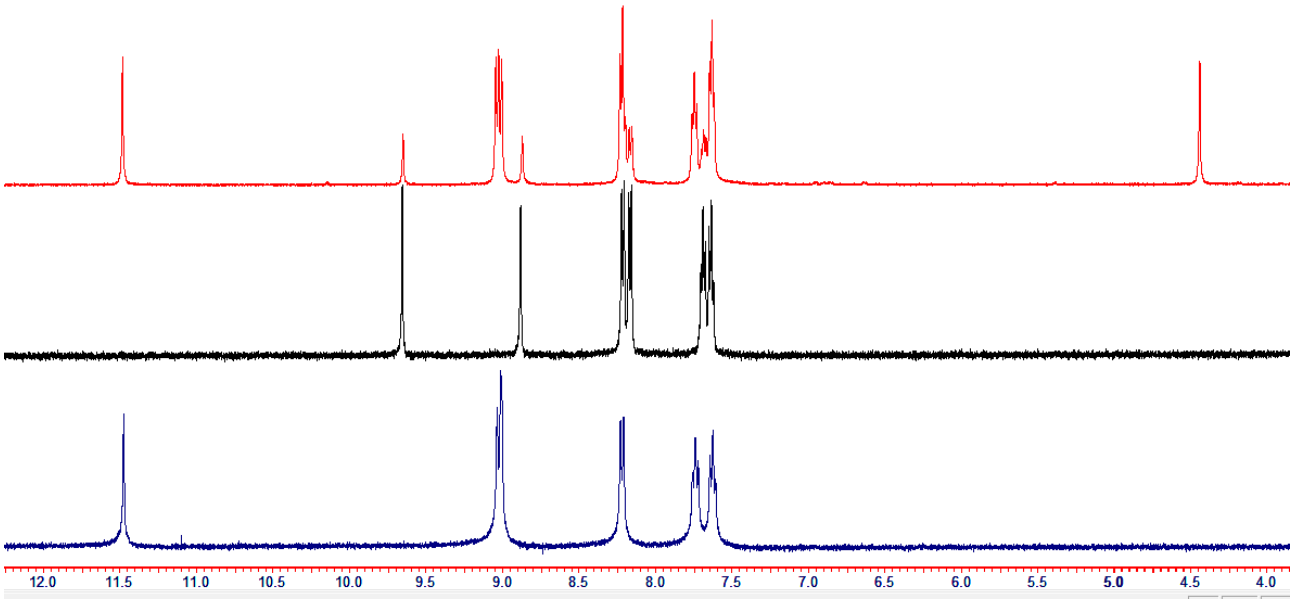

(a)

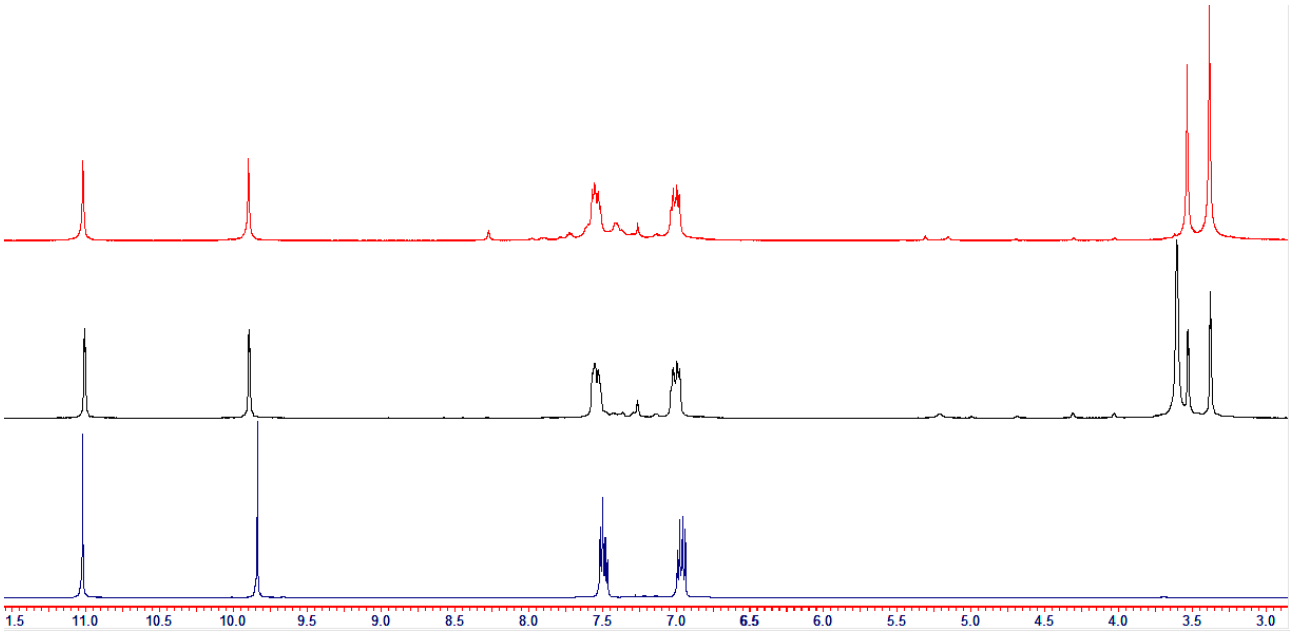

(b)

Fig. S1. (a) ^{1}H NMR spectra of 9-anthracenecarbaldehyde (blue), 2-(9-anthrylmethylene)-malononitrile (black) and reaction mixture after 40h heating with **2** (red).

(b) ^{1}H NMR spectra of salicylaldehyde (blue), reaction mixture after 2h (black) and 40h (red) heating with **2**, respectively.

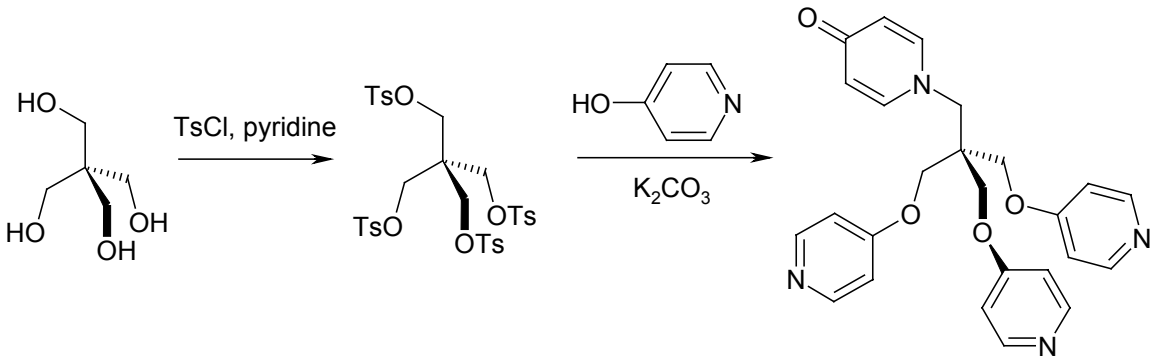

Fig. S2. Scheme, showing synthesis of L^4.

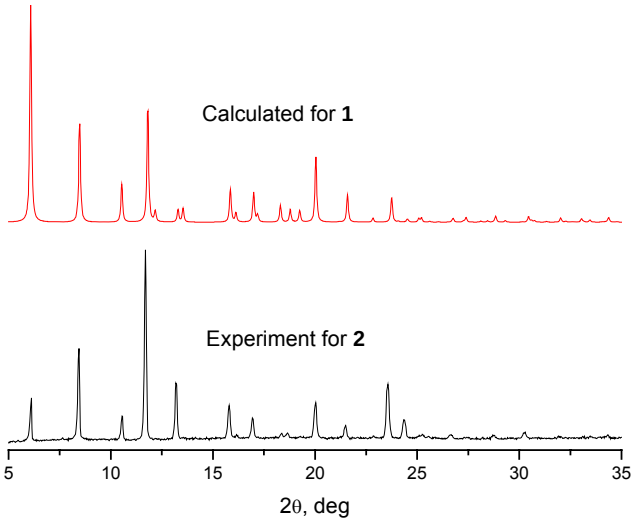

Fig. S3. Powder X-ray diffraction patterns: calculated from X-ray structure for compound **1** (data taken from ref. [1]) and experimental for **2**. λ = 1.54056 Å.

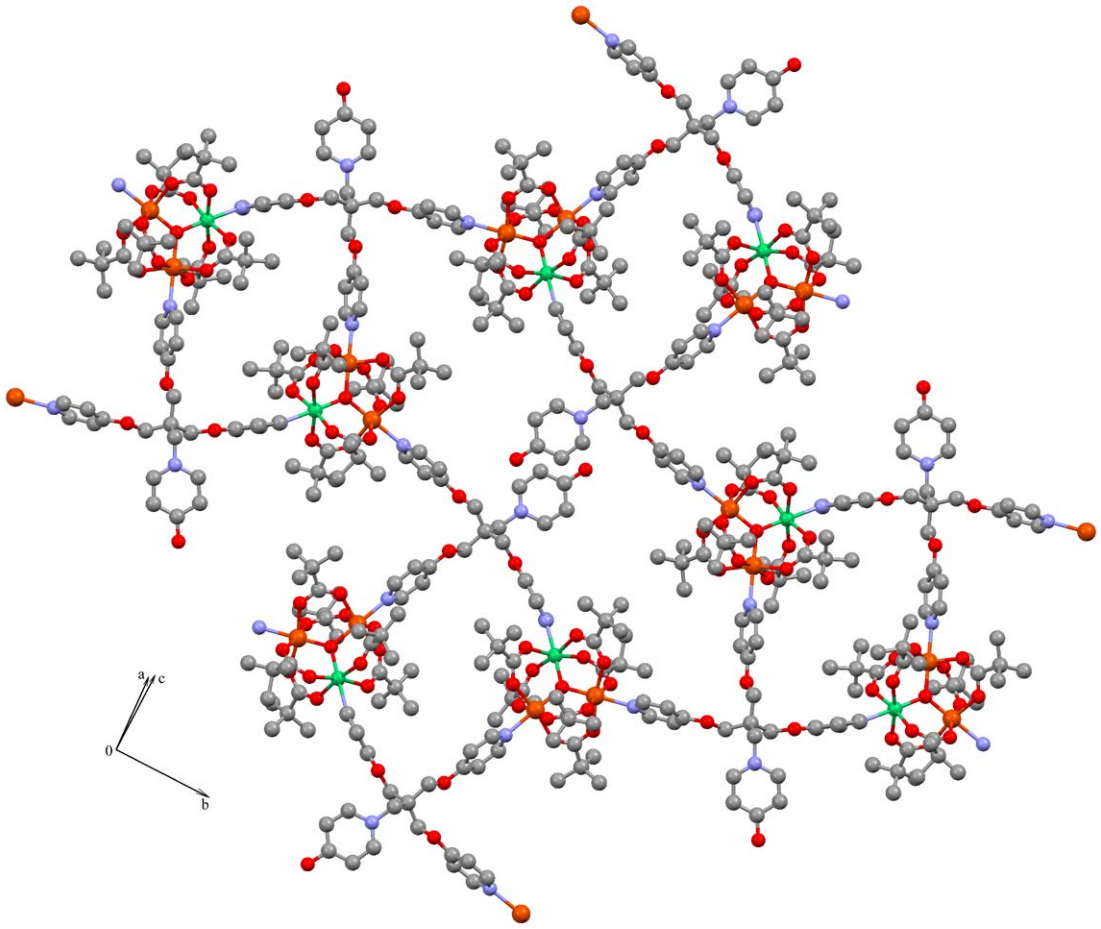

Fig. S4. A fragment of the 2D layer in **4**. Hydrogen atoms and non-coordinated HPiv molecules are omitted for clarity.

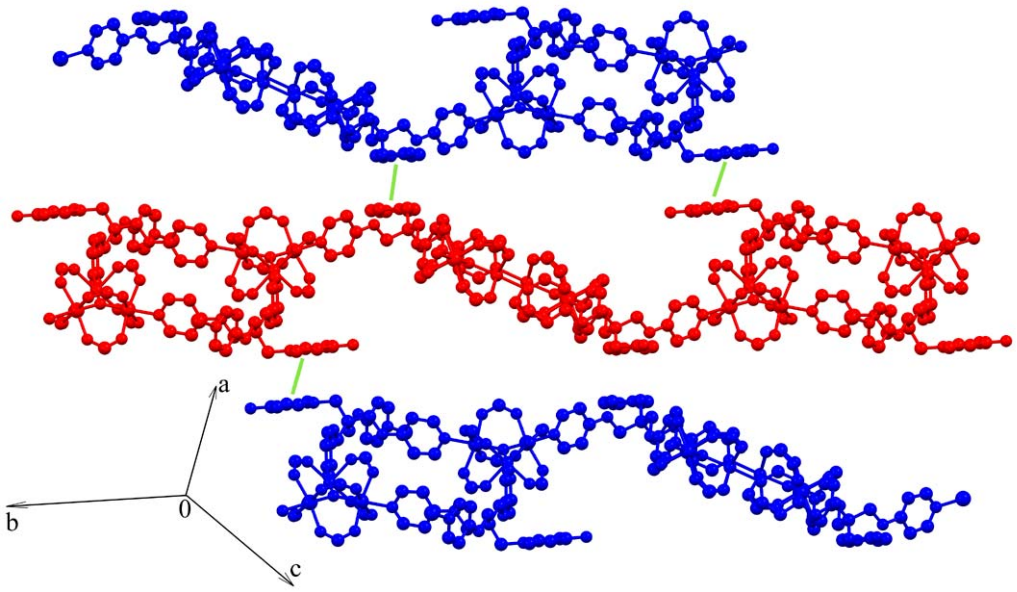

Fig. S5. A fragment of the crystal structure of **4**. Hydrogen atoms, *t*-Bu groups and non-coordinated HPiv molecules are omitted for clarity. Green lines indicate close contacts between adjacent pyridone rings.

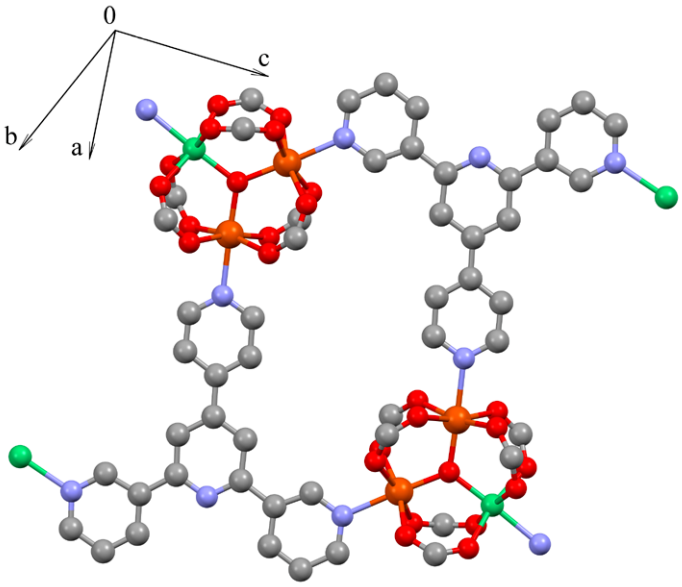

Fig. S6. A fragment of the 2D layer in **3**. Hydrogen atoms and *t*-Bu groups are omitted for clarity.

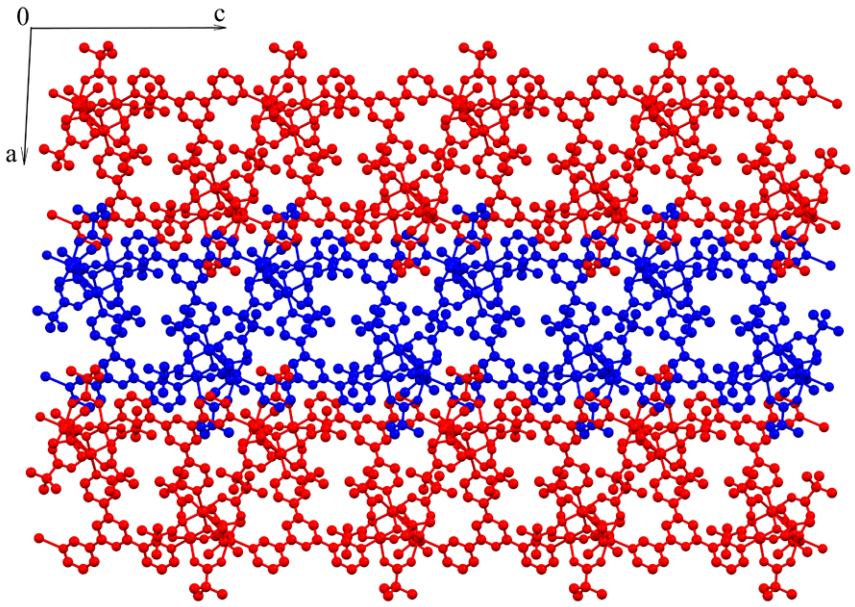

Fig. S7. A fragment of the crystal structure of **3**. Hydrogen atoms are omitted for clarity. Adjacent 2D layers are shown in red and blue.

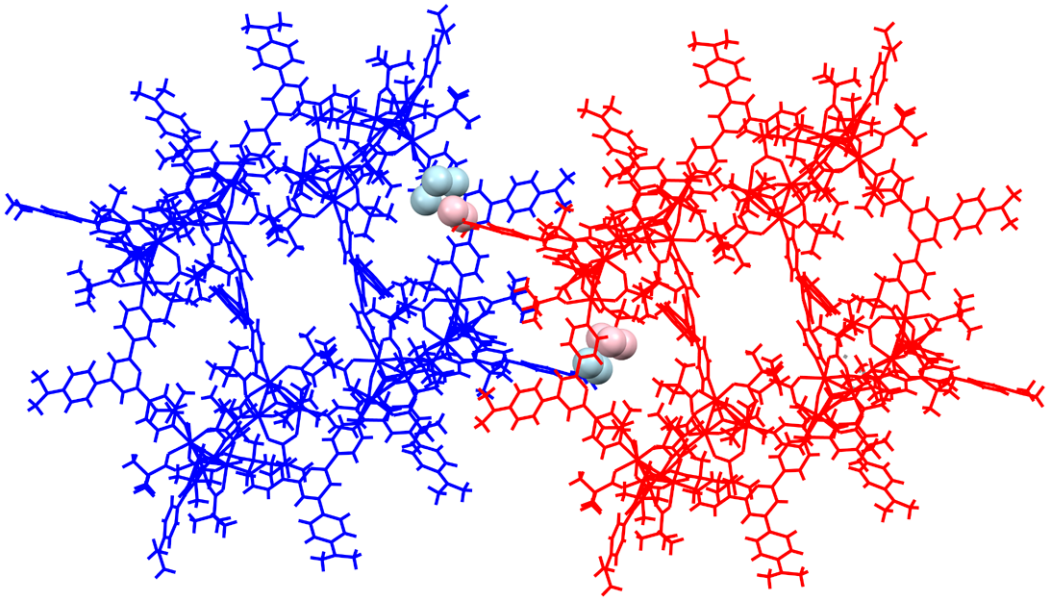

Fig. S8. Visualization of close contacts between H atoms in the crystal structure of $\{Fe_2NiO(Piv)_6\}_8\{L^4\}_{12}$ (**6**). Drawn using data published in.[1]

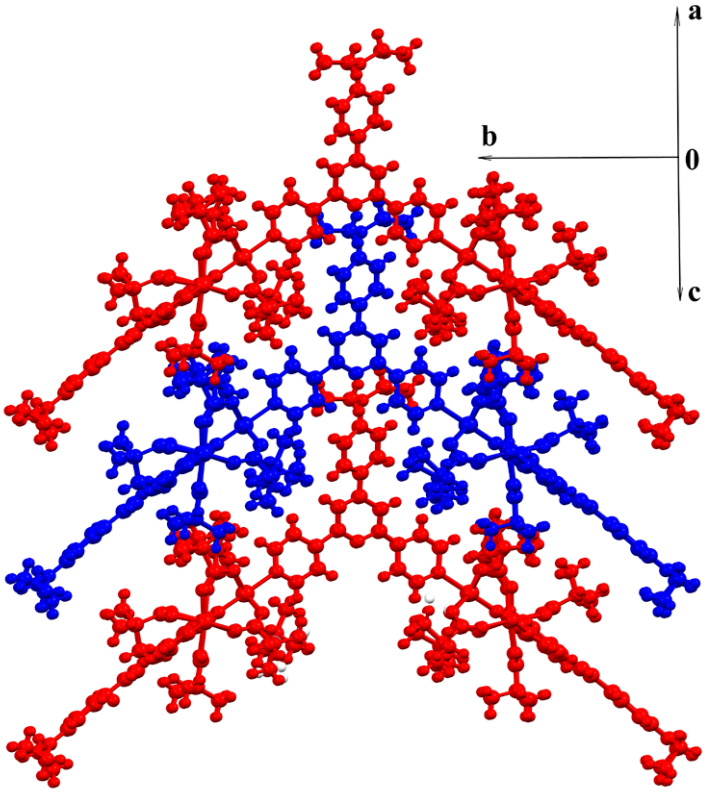

Fig. S9. A fragment of the crystal structure of **5**. Adjacent 2D layers are shown in red and blue. DEF molecules are omitted for clarity.

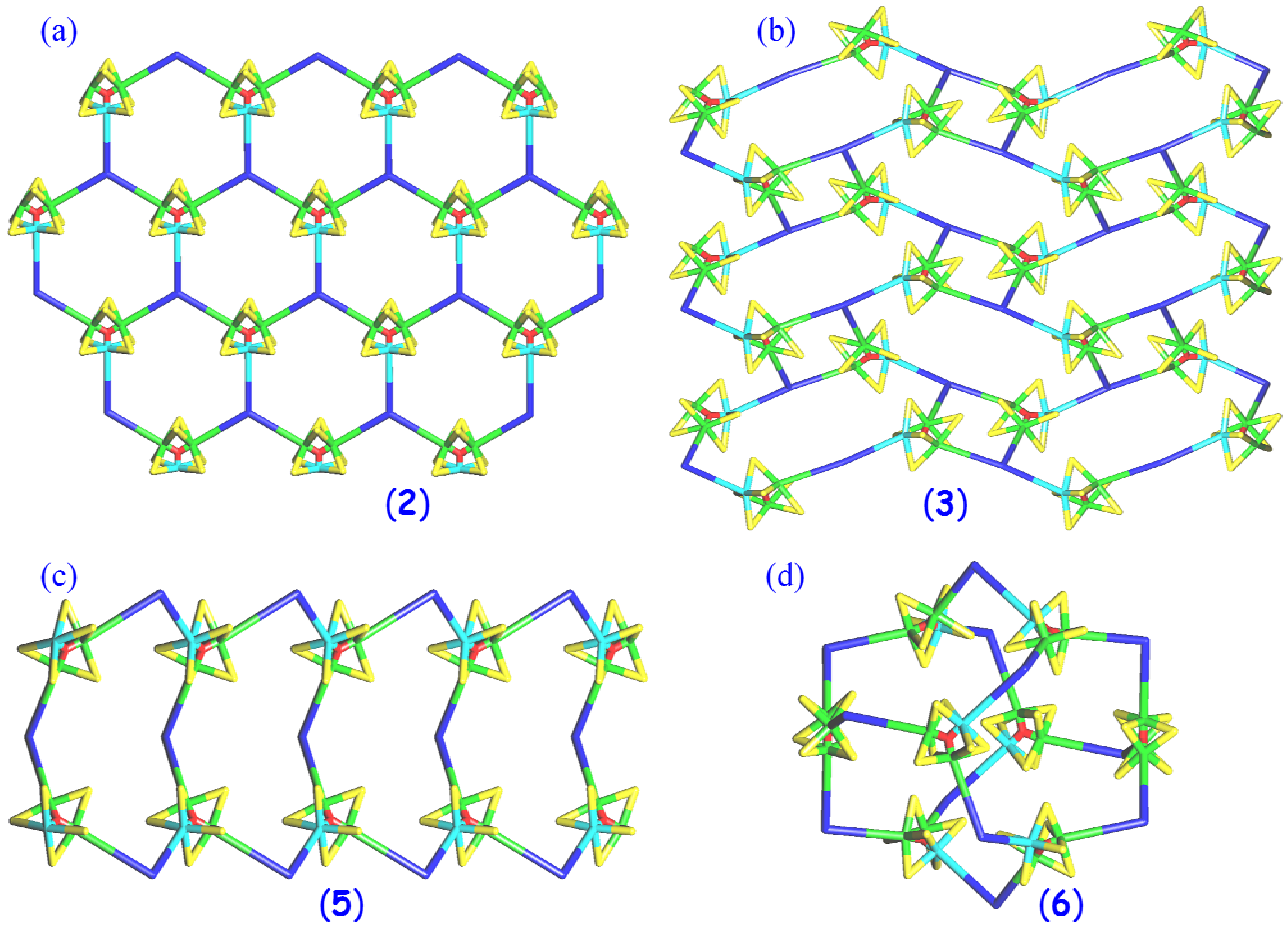

Fig. S10. Topological representations of the underlying networks in **2** (a), **3** (b), **5** (c), and **6** (d) after initial simplification procedure. (a) Trinodal 3,4,4-connected 2D net with the 3,3,4L40 topology and the point symbol of $(3^3.9^2.10)_3(3^3)(9^3)$ (view along the *c* axis). (b) Tetranodal 3,3,4,4-connected 2D layer with the point symbol of $(3^3.12^2.13)(3^3.6.7^2)_2(3^3)(6.12^2)$. (c) Binodal 3,4-connected 0D net with the point symbol of $(3^3.8^2.9)_3(3^3)$. (d) Trinodal 3,3,4-connected 1D chain with the point symbol of $(3^3.8.9^2)_2(3^3.8^2.9)(3^3)$. Networks (b), (c), and (d) are topologically unique and are shown along the *a* axis. Further details: Fe nodes (green), Ni nodes (cyan), μ_3-O nodes (red), centroids of μ_3-$L^{1\text{-}3}$ nodes or μ_2-$L^{5,6}$ linkers (blue).

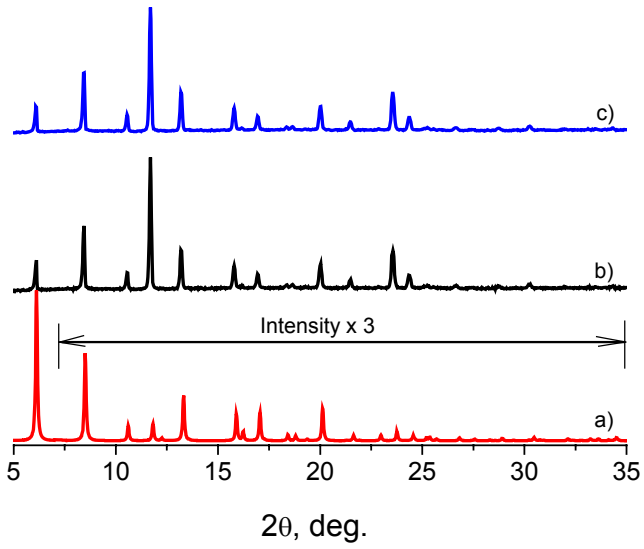

Fig. S11. Powder X-ray diffraction patterns: (a) calculated from X-ray structure for compound **2** at 150 K; (b) experimental for air-dried sample of **2**; (c) experimental for sample of **2** dried in vacuum (10^{-3} Torr). Intensity is re-scaled only for pattern (a). λ = 1.54056 Å.

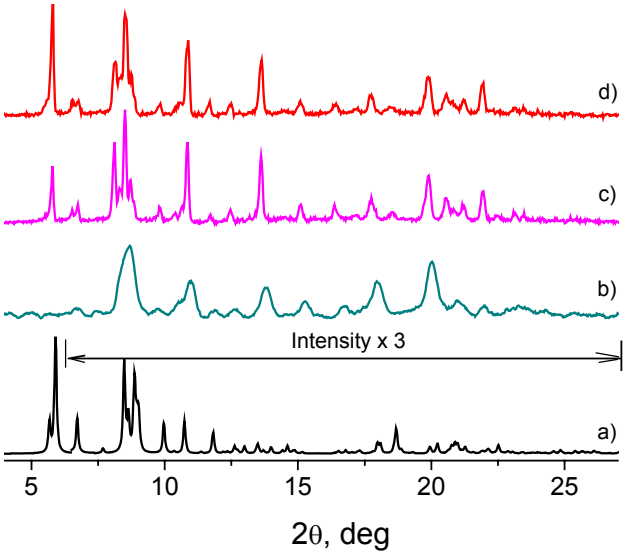

Fig. S12. Powder X-ray diffraction patterns: (a) calculated from X-ray structure for compound **3** at 230 K; (b) experimental for air-dried sample synthesized in DMSO (compound **3**); (c) experimental for air-dried sample synthesized in DMF (compound **3'**); (d) experimental for sample synthesized in DMF (compound **3'**) and dried in vacuum (10^{-3} Torr). Intensity is re-scaled only for pattern (a). λ = 1.54056 Å.

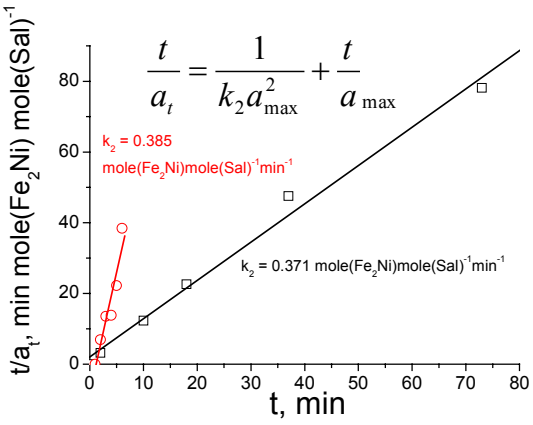

Fig. S13. Fits of salicylaldehyde sorption rate by the second order equation; a_{max} is the maximal sorption capacity, a_t is the sorption capacity at time t, k_2 is the constant of sorption rate.

Table S1. Catalytic activity of selected compounds in reactions of aldehydes condensation with activated methylene-containing compounds.

Catalyst	Aldehyde [a]	Conversion, %	TON [a]	Reaction conditions	Ref.
Malononitrile as active methylene component					
2	Sal	88	80 mol/mol Fe_2Ni	100 °C, 40 h	present work
2	Aca	29	26 mol/mol Fe_2Ni	100 °C, 40 h	present work
L^2	Sal	27	24 mol/mol L^2	100 °C, 40 h	present work
L^2	Aca	10	9 mol/mol L^2	100 °C, 40 h	present work
$Pd_3(mpdm)_3(NO_3)_6$ [b]	Sal	80	7 mol/mol Pd^{2+}	r.t., 3 h	2
$[Tb(tca)\cdot 2DMF]_n$ [c]	Sal	99	50 mol/mol Tb^{3+}	r.t., 6 h	3
$[Cu_3(btc)_2]_n$ [d]	BA	100	6 mol/mol Cu^{2+}	80 °C, 0.5 h	4
Basolite F300 [d]	BA	35	2 mol/mol Fe^{3+}	80 °C, 5 h	4
$[Zr_6O_4(OH)_4(L^7)_6]_n$ [e]	BA	98	11 mol/mol Zr^{4+}	40 °C, 40 min	5
$[Zr_6O_4(OH)_4(L^7)_6]_n$ [e]	Aca	87	10 mol/mol Zr^{4+}	40 °C, 40 min	5
Meldrum's acid as active methylene component					
$[\{Pd(en)\}_6(\mathbf{L^2})_4](NO_3)_{12}$	BA	38 [f]	6 mol/mol Pd^{2+}	r.t., 6 h	6
$[\{Pd(en)\}_6(\mathbf{L^2})_4](NO_3)_{12}$	Aca	63 [f]	11 mol/mol Pd^{2+}	r.t., 96 h	6
1,3-dimethylbarbituric acid as active methylene component					
$[\{(tmen)Pd\}_7(timb)_2\times$ $\times(tim)_2](NO_3)_{14}$	BA	69 [g]	1 mol/mol Pd^{2+}	r.t., 4 min	7
$[\{(tmen)Pd\}_7(timb)_2\times$ $\times(tim)_2](NO_3)_{14}$	Aca	35 [g]	0.5 mol/mol Pd^{2+}	r.t., 72 h	7

[a] TON values were calculated as TON = $(\alpha\times\upsilon_0)/(100\%\times\upsilon_{\text{active sites}})$, where α is conversion of aldehyde (%), υ_0 is initial amount of aldehyde (mol), $\upsilon_{\text{active sites}}$ is amount of active sites (mol). Abbreviations of aldehydes: Sal = salicylaldehyde, BA = benzaldehyde, Aca = 9-anthracenecarbaldehyde.

[b] 4 mol % of catalyst; mpdm = 3,3',5,5'-tetra[N-(4-pyridyl)methylcarboxylamide]diphenylmethane;

[c] 2 mol % of catalyst; (H_3tca − tricarboxytriphenylamine);

[d] 5.5 mol % of $[Cu_3(btc)_2]_n$ and 5.4 mol % of Basolite F300, respectively; H_3btc is 1,3,5-benzenetrixarboxylic acid. Basolite F300 is Fe complex of 1,3,5-benzenetricarboxylate, its structure was not unambiguously determined.[8] Concentration of Basolite F300 and TON values re-calculated per formula $[Fe_3O(OH)(btc)_2]_n$;

[e] 1.5 mol % of catalyst; L^7 = 2-amino-1,4-benzenedicarboxylate;

[f] 1 mol % of catalyst;

[g] 10 mol % of catalyst; tmen = N,N,N',N'-tetramethylethylenediamine, timb = 1,3,5-tris(1-imidazolyl)benzene, tim = 1,2,4,5-tetrakis(1-imidazolyl)benzene.

References for Supporting Information

1. V. N. Dorofeeva, S. V. Kolotilov, M. A. Kiskin, R. A. Polunin, Z. V. Dobrokhotova, O. Cador, S. Golhen, L. Ouahab, I. L. Eremenko, V. M. Novotortsev *Chem. Eur. J.,* **2012***,* 18, 5006 – 5012.
2. Liu, Y.; Zhang, R.; He, C.; Dang, D.; Duan, C. *Chem. Commun.* **2010**, 46, 746–748.
3. Wu, P.; Wang, J.; Li, Y.; He, C.; Xie, Z.; Duan, C. *Adv. Funct. Mater*. **2011**, 21, 2788–2794.
4. Opanasenko, M.; Dhakshinamoorthy, A.; Shamzhy, M.; Nachtigall, P.; Horáček, M.; Garcia, H.; Čejka, J. *Catal. Sci. Technol.* **2013**, 3, 500–507.
5. Yang, Y.; Yao, H.-F.; Xi, F.-G.; Gao, E.-Q. *J. Mol. Cat. A: Chem.* **2014**, 390, 198–205.
6. Murase, T.; Nishijima, Y.; Fujita, M. *J. Am. Chem.Soc.* **2012**, 134, 162−164.
7. Samanta, D.; Mukherjee, P. S. *Chem. Comm.* **2013**, 49, 4307–4309.
8. Nakhla, J. *Aldrich ChemFiles* **2009**, 9.2, 19.